

***In vitro* nifedipine release from poly(lactic acid)/chitosan nanoparticles loaded with nifedipine**

Nguyen Thuy Chinh,¹ Nguyen Thi Thu Trang,¹ Nguyen Vu Giang,¹ Dinh Thi Mai Thanh,¹
To Thi Xuan Hang,¹ Nguyen Quang Tung,² Chu Quang Truyen,³ Pham Minh Quan,³ Pham Quoc Long,³
Thai Hoang¹

¹Institute for Tropical Technology, Vietnam Academy of Science and Technology, Building A13, 18 Hoang Quoc Viet, Cau Giay, Postal Code+84 Hanoi, Vietnam

²Hanoi University of Industry, Minh Khai Commune, Tu Liem, Postal Code+84 Hanoi, Vietnam

³Institute of Natural Products Chemistry, Vietnam Academy of Science and Technology, Building 1H, 18 Hoang Quoc Viet, Cau Giay, Postal Code+84 Hanoi, Vietnam

Corresponding authors: N. T. Chinh (E-mail: thuychinhhn@gmail.com) and T. Hoang (E-mail: hoangth@itt.vast.vn)

ABSTRACT: In this study, nanoparticles based on poly(lactic acid) (PLA), chitosan (CS), and nifedipine (NIF) were prepared by an emulsion method with poly(ethylene oxide) (PEO) as an emulsifier. We investigated the most suitable conditions for preparing the poly(lactic acid)/chitosan/nifedipine nanoparticles (PCNs) by changing the distilled water volume, PEO content, and PLA/CS ratio. NIFs with different contents were loaded into poly(lactic acid)/chitosan nanoparticles (PCs) to study *in vitro* drug-delivery systems. The PCNs were characterized with a Zetasizer particle size analyzer, field emission scanning electron microscopy, Fourier transform infrared (FTIR) spectroscopy, and X-ray diffraction (XRD) methods. From the obtained results of the particle size parameters of the PCNs, the most suitable conditions for the preparation of the PCNs were found. The FTIR spectroscopy and XRD results show that NIF was loaded into the PCs. The PCNs had major basic particle sizes in the range 20–40 nm. NIF release from the PCNs was studied as a function of the pH of the immersed solution, the immersion time, and the NIF content. The kinetics of drug release were investigated and are reported to determine the type of release mechanism. © 2016 Wiley Periodicals, Inc. *J. Appl. Polym. Sci.* **2016**, *133*, 43330.

KEYWORDS: biopolymers and renewable polymers; drug-delivery systems; kinetics; nanostructured polymers

Received 28 July 2015; accepted 8 December 2015

DOI: 10.1002/app.43330

INTRODUCTION

Nifedipine (NIF), whose scientific name is dimethyl 2,6-dimethyl-4-(2-nitrophenyl)-1,4-dihydropyridine-3,5-dicarboxylate, is a pharmaceutical/calcium antagonist of the dihydropyridine group, and it has the effect of selective inhibition. NIF, which has a very low solubility and is biodegradable in photochemical reactions, is used in the treatment of angina pectoris and hypertension.¹ Its biological half-life is about 2 h, and it is eliminated rapidly. Therefore, repeated daily administration is necessary to maintain effective plasma levels. NIF has a low and irregular bioavailability of about 50% after oral administration with a high first-pass effect. Drugs with biological half-lives in the range 2–8 h have been suggested as good candidates for sustained-release formulations.¹

The investigation of long-circulating systems based on biopolymers and NIF has recently been considered by researchers.^{2–7} Thanks to the controlled drug release of these systems by changes in the polymer–drug ratio, particle size distribution,

type of solvent, concentration, and nature of emulsifier, fabricated temperatures can help to overcome the disadvantages of NIF, including its short half-life, low solubility, and easy release in different pH solutions.

There have been some articles on the results of *in vitro* NIF release and release kinetics from biopolymer microspheres with loaded NIF. In research published in 1996, Filipović-Grčić *et al.*² investigated the *in vitro* release NIF from chitosan (CS) microspheres of NIF and NIF–cyclodextrin inclusion complexes. The obtained results show that the *in vitro* release rates were influenced by the crosslinking density, particle size, and initial drug loading in the microspheres and that the mechanism of NIF release complied with Higuchi's square root of time models. Jingjun *et al.*³ prepared microparticles of an ammoniomethacrylate copolymer (RL) and ethyl cellulose (EC) binary blend containing NIF with different RL/EC weight ratios. A drug-release study indicated that NIF release from the microparticles reached 25–80% after 6 h for samples prepared at different RL/EC

weight ratios and followed a Fickian diffusion mechanism. Guyot and Fawaz⁴ showed that the NIF incorporation efficiency in EC microspheres decreased when the organic phase viscosity was increased. All of the microsphere formulations exhibited slow and S-shaped release profiles with a poor dissolution efficiency, and the rate of drug release was slightly influenced by the initial NIF loading. NIF release from the microspheres was well described by combined kinetics (zero- and first-order kinetics or zero-order and Higuchi square-root kinetics).⁴ Praveen et al.⁵ also studied the *in vitro* release kinetics of NIF from microspheres of poly(vinyl alcohol) and succinyl chitosan. As per the Korsmeyer–Peppas equation, the estimated value of the diffusional constant that characterizes the drug-release-transport mechanism (n) for microspheres indicated a swelling-controlled release mechanism (non-Fickian). Namdev et al.⁶ synthesized poly(sebacic anhydride-co-Pluronic F68/F127) biopolymeric microspheres for the controlled release of NIF in the size range 10–50 μm . The percentage cumulative release data from microspheres observed for 4 h of dissolution in pH 7.4 phosphate buffer were 18–33%, and the release kinetic data according to the power law equation displayed the anomalous nature of NIF release from the matrices ($n < 0.5$). The NIF release kinetics from microspheres of copolymeric *N*-vinylpyrrolidone and 2-ethoxyethyl methacrylate was also suggested according to the Fickian trend. It was clear that *in vitro* NIF release and NIF release kinetics were mainly applicable in microsize systems based on polysaccharide.

Poly(lactic acid) (PLA) is one of the most widely components of polymer nanoparticles (PNs) because of its biocompatibility, biodegradability, renewability, and excellent incorporation capability for hydrophilic drugs.⁸ However, the high crystallinity, strong hydrophobicity, and especially, lack of bioactive functions of PLA often result in an uncontrollable biodegradation rate and an undesirable biological response to cells and/or tissues.⁸ Therefore, the combination of bioactive functions, such as biocompatibility, biodegradability, nontoxicity, and low cost, of CS with the good properties of PLA to express a new kind of biohybrid amphiphile and to develop long-circulating systems is promising.^{8,9} Poly(lactic acid)/chitosan nanoparticle (PCs) has been applied to load some drugs except for NIF; these drugs include anthraquinone,⁸ rapamycin,¹⁰ paclitaxel,¹¹ ketoprofen,¹² lamivudine,¹³ rifampicin,¹⁴ and bone morphogenetic proteins (BMP)-2-derived synthetic peptide.¹⁵ The emulsion method is one of the most popular methods for preparing PCs loaded with different drugs.^{8,11–14}

Until now, literature on the preparation of PCs loaded with NIF and the investigation of NIF release from PCs has not been published. The aim of this study was to determine the *in vitro* NIF release and drug-release kinetics from poly(lactic acid)/chitosan/nifedipine nanoparticles (PCNs) prepared by the emulsion method. In addition, suitable preparation conditions of the PCNs and their characteristics, such as particle size distribution, structural morphology, and crystallinity, were also investigated and are discussed.

EXPERIMENTAL

Materials

PLA (in pellets, degree of hydrolyzing > 99%, density = 1.25 g/cm³, molecular weight = 1.42×10^4 Da, melt flow index = 7.75 g/10 min at 210 °C, 2.16 kg), CS (degree of deacetylation > 77%,

viscosity = 1220 cP, 1.61×10^5 Da), poly(ethylene oxide) [PEO; volume-average molecular weight = 100,000, glass temperature = -67.0 °C, polydispersity index (Weight-average molecular weight/Number-average molecular weight) = 1.02–1.12], and NIF (in powder, purity \geq 98%, yellow color) were obtained from Sigma-Aldrich. Dichloromethane, acetic acid, hydrochloric acid, and phosphate buffer solutions were analytical reagents and were used without further purification.

Preparation of the PCNs

PCNs were prepared by an emulsion method according to following steps: PLA was dissolved in dichloromethane (O solution), NIF was dissolved in ethanol (W1 solution), and CS and PEO were dissolved in a 1% acetic acid solution (W2 solution). (The weights of the components were calculated, as shown in Table I.) Next, W1 solution was poured into O solution and ultrasonically stirred to form a W1/O mixed solution. Thereafter, the W2 solution was poured into the W1/O mixed solution and then sonicated three times for 5 min. A volume of 100 mL of distilled water was added to the W1/O/W2 mixed solution. The previous mixed solution was ultrasonically stirred and cooled with ice. The PCNs were collected by centrifugation and then washed three times to remove excessive emulsifier by water before they were lyophilized in a FreeZone 2.5 machine (Labconco). The obtained nanoparticles were abbreviated as listed in Table I.

Characterization

Fourier transform infrared (FTIR) spectroscopy was used to characterize the structure of the PLA, CS, NIF, PCs, and PCNs. We recorded their FTIR spectra on a Nicolet/Nexus 670 spectrometer at room temperature in the wave-number range 400–4000 cm⁻¹ and averaged 16 scans with a resolution of 4 cm⁻¹. The mean diameter and size distribution of the nanoparticles were measured by a Zetasizer version 6.20 particle size analyzer (Malvern Instruments, Ltd.). The morphology of the nanoparticles was analyzed with an S-4800 field emission scanning electron microscopy (FESEM) instrument (Hitachi). A Siemens D5000 X-ray diffractometer with Cu K α radiation ($\lambda = 0.154$ nm) at a generator voltage of 40 kV, and a current of 30 mA was used to determine the crystalline degree of NIF and the PCNs. The X-ray diffraction (XRD) data were collected between 5 and 60° at room temperature at a scanning speed of 0.7°/s and step size of 0.03°.

In Vitro Drug-Release Studies

The *in vitro* NIF release test from the PCNs was carried out as follows: 50 mg of each sample was immersed in 500 mL of phosphate buffer solution (pH 6.8 and 7.4) or HCl solution (pH 1.2 and 2.0) at 37 °C and placed in an incubated shaker at 120 rpm. At predetermined time intervals, 3-mL aliquots were withdrawn, and the concentration of released NIF was monitored by UV spectroscopy (CINTRA 40, GBC).

The dissolution medium was replaced with fresh buffer solution to maintain the total volume. The NIF release percentage was determined by the following equation:

$$\text{Drug release (\%)} = C_{(t)} / C_{(0)} \times 100$$

where $C_{(0)}$ and $C_{(t)}$ represent the amount of NIF loaded and the amount of drug released at time t , respectively. All studies were done in triplicate.

Table I. Recipes for the Preparation of the PCNs and the Corresponding Particle Size Diameters

Sample	Distilled water volume (mL)	PEO content (mg)	PLA/CS ratio	NIF content (wt %) ^a	Size (d nm)
PCN50W	50	400	2:1	20	203.7 ± 7.5
PCN100W	100	400	2:1	20	163.3 ± 11.9
PCN200W	200	400	2:1	20	181.6 ± 13.3
PCN250W (or PCN20N)	250	400	2:1	20	115.8 ± 8.3
PCN300W	300	400	2:1	20	229.4 ± 9.5
PCN200E	250	200	2:1	20	241.1 ± 18.6
PCN600E	250	600	2:1	20	241.1 ± 16.6
PCN11R	250	400	1:1	20	178.0 ± 11.6
PCN12R	250	400	1:2	20	405.7 ± 32.4
PCs	250	400	2:1	0	390.3 ± 64.1
PCN10N	250	400	2:1	10	187.3 ± 27.2 (94.2%) 68.0 ± 4.0 (5.8%)
PCN30N	250	400	2:1	30	141.0 ± 25.6
PCN50N	250	400	2:1	50	196.1 ± 33.9 (95.2%) 56.6 ± 4.5 (4.8%)

^aIn comparison with PLA weight.

RESULTS AND DISCUSSION

Suitable Preparation Conditions for the PCNs

To investigate the influence of the volume of distilled water added to W1/O/W2 mixed solution on the particle size distribution of the PCNs, the samples were prepared by an emulsion method with different water volumes from 50 to 300 mL. Figure 1 demonstrates the particle size distribution diagrams of PCN50W, PCN100W, PCN200W, PCN250W, and PCN300W. We observed that the particle size of all of the samples changed in the range 70–350 nm. The average particle size reached a minimum value at 115.8 ± 8.3 nm, which corresponded to PCN250W, and a maximum value at 229.4 ± 9.5 nm, which corresponded to PCN300W (see Table I). The differences in the particle size distribution of the previous samples may have been caused by the interaction between water and the drug and water and the polymer. From the obtained results, it was clear that the suitable distilled water volume for the preparation of the PCNs was 250 mL.

Similarly, because of the results of the particle size distribution of the samples with different PEO contents and PLA/CS ratios, the most suitable parameters for the preparation of PCNs with a minimum particle size were 400 mg of PEO and a PLA/CS ratio of 2:1 (see Table I).

The previous suitable conditions were applied to prepare PCNs with different loaded NIF contents from 10 to 50 wt %. The particle sizes of these samples are also listed in Table I. The average particle size of these samples was from 115 to 196 nm. In comparison with PCs loaded with some other drugs as mentioned in the literature,^{8,10,13,14} the obtained PCNs had quite small particle sizes. Interestingly, all of the PCNs had particle sizes smaller than those of the PCs. This means NIF played an important role in the improvement size distribution of the PCNs. This could be explained by the fact that the emulsion

method is appropriate for the formation of polymer nanoparticles carrying hydrophilic drugs such as NIF.^{8,13,14} The C=O, C–O, NH, and NO₂ groups in NIF could interact with the C–O, NH, and OH groups in CS and the C=O, C–O, and OH groups in PLA through hydrogen-bonding and dipole–dipole interactions as suggested in Figure 2 and discussed later in the FTIR analysis.

FTIR Spectra

The FTIR spectra of the PCNs almost exhibited the characteristic groups of both the NIF and PCs (see Table II and Figure 3). The FTIR spectrum of NIF indicated characteristic peaks of the stretching vibrations of N–H groups at 3469 cm^{-1} and CH (aromatic) groups at 3330 cm^{-1} . The peaks were placed at 2952, 2923, 2849, 1433, and 1380 cm^{-1} corresponded to the

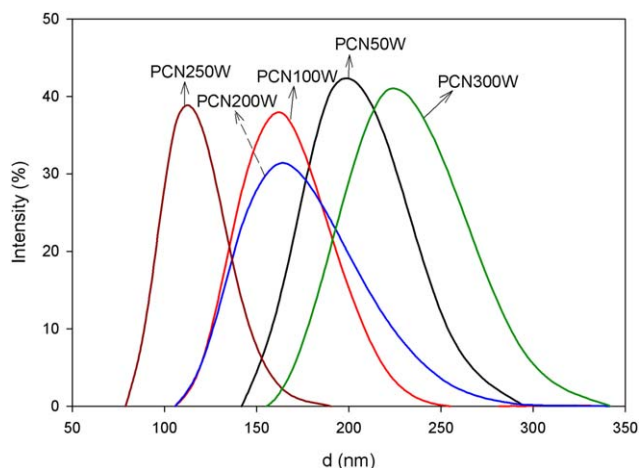


Figure 1. Particle size distribution diagrams of PCNs prepared with different water volumes, where d is diameter. [Color figure can be viewed in the online issue, which is available at wileyonlinelibrary.com.]

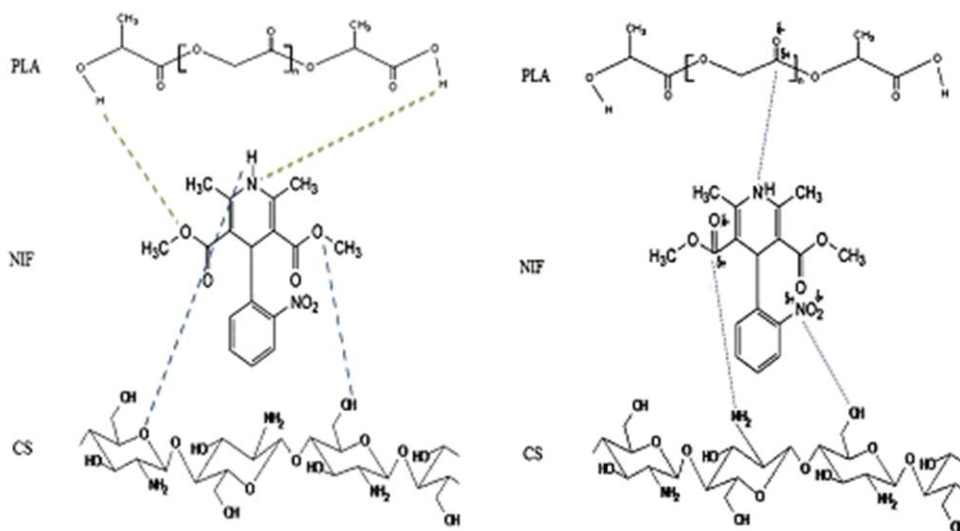


Figure 2. Hydrogen-bond (left) and dipole–dipole interactions (right) between NIF, PLA, and CS. [Color figure can be viewed in the online issue, which is available at wileyonlinelibrary.com.]

asymmetrical stretching, symmetrical stretching, and bending vibrations of ethyl, C–H, and methyl groups, respectively.^{7,16} The characteristic peak at 1683 cm^{-1} was ascribed to ester carbonyl stretching vibrations, whereas the peak at 1641 cm^{-1} and the absorption region at $792\text{--}857\text{ cm}^{-1}$ were attributed to the stretching and bending vibrations of the C=C group in the benzene ring. In addition, some of characteristic peaks at 1529 and 1496 cm^{-1} were due to the bending vibrations of the NH and NO₂ groups. Moreover, the symmetrical and asymmetrical stretching vibrations of C–O–C were also found at 1118 and

1226 cm^{-1} , respectively. The intensity of the characteristic peaks of CH (aromatic), C=O (ester), and NO₂ groups in the FTIR spectra of the PCNs increased significantly when the NIF content increased. These groups were not observed in the FTIR spectra of the PCs, whereas a new peak corresponding to the stretching vibrations of carbonyl groups in the acid moiety was located at 1759 cm^{-1} .⁸

A decrease in the intensity and shifts in the characteristic peaks for the stretching vibrations of C=O (acid) and C–O and bending vibrations of NH in the spectra of PCNs were also

Table II. FTIR Characteristics of the NIF, PCs, and PCNs

Vibration	Wave numbers (cm^{-1})					
	NIF	PCs	PCN10N	PCN20N	PCN30N	PCN50N
$\nu\text{--NH}_2, \nu\text{OH (broad)}$	3469	3445	3436	3441	3440	3428
$\nu\text{CH(aro)}$	3330	—	—	3329	3334	3334
$\nu\text{CH,CH}_2$	2952	2997	3001	3001	3000	2999
	2923	2920	2951	2948	2950	2951
νCH_3	2849	2849	—	—	—	2852
$\nu\text{C=O (acid)}$	—	1759	1760	1759	1759	1758
$\nu\text{C=O (ester)}$	1683	—	—	1685	1684	1684
$\nu\text{C=C (aro)}$	1641	—	1626	1623	1627	1628
$\delta\text{--NH}$	1529	—	1533	1530	1531	1530
$\delta\text{--NO}_2$	1496	—	—	1496	1497	1497
$\delta\text{CH, CH}_2$	1433	1460	1458	1456	1456	1455
δCH_3	1380	1386	1384	1360	1354	1351
$\nu\text{C--O--C}$	1226	1189	1189	1189	1188	1225
	1118	1093	1091	1092	1091	1188
						1092
$\delta\text{C=C (aro, multi peaks)}$	857	—	—	869	866	865
	829	—	—	825	829	831
	792	—	—	—	—	792

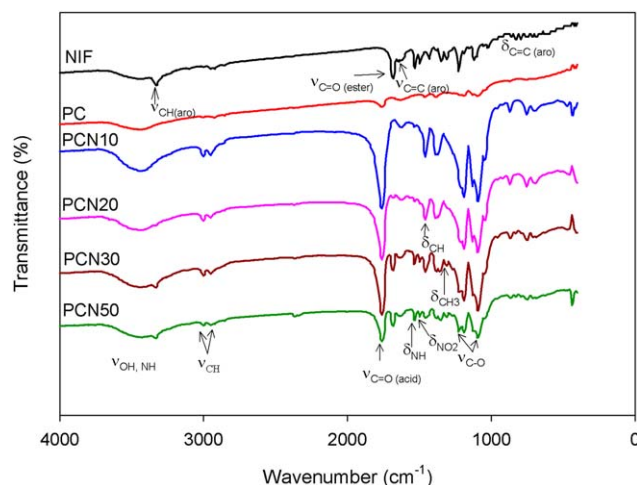


Figure 3. FTIR spectra of the NIF, PC, and PCNs. [Color figure can be viewed in the online issue, which is available at wileyonlinelibrary.com.]

observed. This could be explained by hydrogen-bonding and dipole–dipole interactions between PLA, CS, and NIF, as mentioned previously. Interactions between the polymer and drug have also been shown by some other researchers.^{8,13}

Surface Morphology

Figure 4 displays the surface morphology of the PCs and PCN250W. The FESEM images showed that both the PCs and PCN250W mainly had a spherical morphology with basic particle sizes of about 20–40 nm. However, the particles were agglomerated together, and this led to the formation of a bigger, agglomerated particle size. Therefore, the observed particle size from the previous size distribution diagram was in agreement with the results from the FESEM images. The surface morphology of the NIF-loaded PCs was the same for the sample prepared without NIF, but the particles in the PCNs dispersed more separately and regularly than those in the PCs because of the interactions between NIF, PLA, and CS, as reported elsewhere.^{8,13}

XRD

Figure 5 shows the XRD diagrams of the NIF, PCs, and PCNs. The XRD diagram of NIF showed strong crystalline peaks at 2θ s of 16, 19.56, and 24.55 Å.^{3,6,17} Two broad crystalline peaks were found at 2θ s of 16.59 and 19.01 Å; these peaks corresponded to the (200) and (110) planes typical of orthorhombic

crystals of PLA and CS, respectively, in PCs. These results were similar to those of Nanda *et al.*,¹¹ Silverajah *et al.*¹⁸ and Ioelovich.¹⁹

The XRD diagrams of the PCNs indicated a slight shift, and the intensities of the crystalline peaks increased remarkably in comparison with the crystalline peak of the PCs. For instance, the crystalline peaks were found at 2θ s of 16.62, 16.71, 16.57, and 16.53 Å for PCN10N, PCN20N, PCN30N, and PCN50N, respectively. This means that the crystallinity of the PCNs was higher than that of the PCs and that NIF, PLA, and CS interacted with each other. With increasing NIF content in the PCNs, the intensities of the crystalline peaks of NIF increased clearly. In contrast, the crystalline peaks of PLA and CS became broader, and the intensities of these peaks decreased. This led to a reduction in the relative crystallinity of the PCNs.

In Vitro Drug Release

Setting Calibration Equation of NIF in Different pH Solutions. The calibration equation of NIF in solutions of pH 1.2 and 2.0 (corresponding to the lower portion of the stomach, where products stay from 1 to 3 h), 7.4 (corresponding to the duodenum region in the body, where products stay from 30 to 60 min), and 6.8 (corresponding to the colon region in the body, where products stay from 10 to 15 h) were set up with the data from the UV–visible spectra. The calibration equations and regression coefficients (R^2) were calculated by Excel software, in which x and y were concentration of NIF and the optical absorbance, as shown in Table III. The obtained results show that all of the R^2 were higher than 0.996. Therefore, these calibration equations were applied to determine the released NIF content from the PCNs in the previous pH solutions.

Determination of the Drug-Loading Efficiency. The drug loading was determined as follows: PCNs were dissolved in ethanol, NIF was separated easily from PCN, and then, the solution containing NIF was used to determine the UV–visible spectra.² On the basis of the calibration equation of NIF in ethanol solvent, the drug loading in the PCNs was calculated. The obtained results were concentrations of 98.7, 98.3, 99.0, and 88.6 wt % for PCN10N, PCN20N, PCN30N, and PCN50N, respectively. Noticeably, when the drug content was increased to 50 wt %, the drug-loading efficiency decreased. In general, a lower drug-loading efficiency was observed with a higher drug composition.²⁰

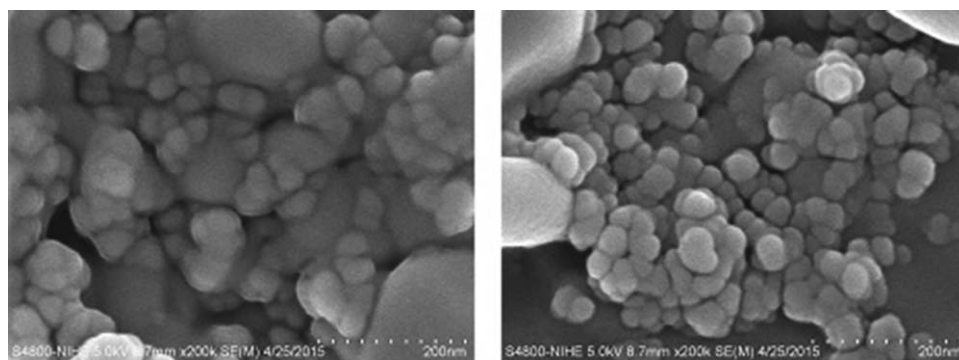


Figure 4. FESEM image of the PCs (left) and PCN250W (right).

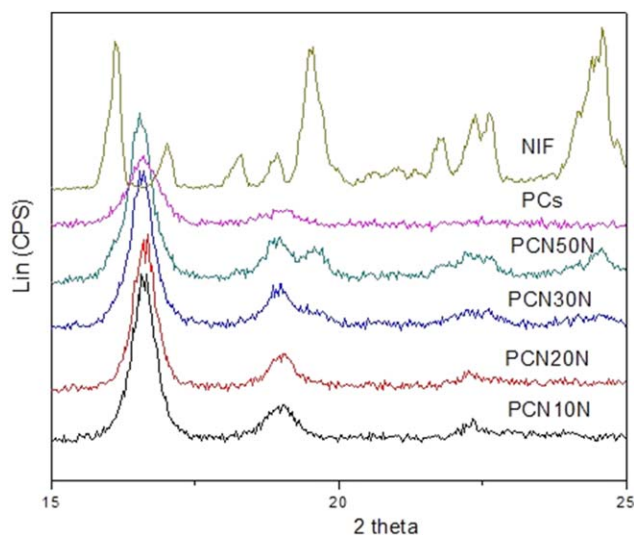


Figure 5. XRD diagrams of NIF, PCs, and PCNs. Lin (CPS), counts per second. [Color figure can be viewed in the online issue, which is available at wileyonlinelibrary.com.]

In Vitro Drug-Release Study. Effect of the pH. To investigate the effect of pH on the drug release from the PCNs, the drug-release contents at pHs of 1.2, 2.0, 6.8, and 7.4 were measured and are shown in Figure 6. We observed that the drug content released from at PCN loadings of 10, 20, 30, and 50 wt % of NIF depended on the solution pH. The drug-release contents in solutions of different pH were in the order according to pH: $7.4 > 6.8 > 2.0 \approx 1.2$. Similar observations were also reported by some other researchers^{8,11,13,14} for PCs loaded with other drugs. For example, in pH 7.4, the NIF release content went up more than 57 wt % after 8 h for the tested samples, whereas at pH 6.8, 2.0, and 1.2, the release contents were 54, 35, and 35 wt %, respectively. This was explained by the repulsion between H^+ ions (in acidic pH) and cations on the surface of CS; this slowed down the hydrolysis of the polymer.¹³ These results indicate that NIF in the nanoparticles is more suitable for the basic environment of the large intestine, colon, and rectal mucosa than for the acidic environment, as indicated in other research.^{13,14}

Effect of the time. Observably, the drug-release content increased according to the testing time. The drug-release rate was initially rapid and then slowed after some hours; this was consistent with phenomena reported by other authors.^{8,11–14,19} The drug-release process included two steps: immediate release

Table III. Calibration Equations and R^2 s of NIF in Solutions of Different pH

pH	λ_{max}	Calibration equation	R^2
1.2	232	$y = 21748x + 0.0514$	0.9962
2.0	220	$y = 32584x + 0.0104$	0.9961
6.8	227	$y = 29913x + 0.0189$	0.9966
7.4	230	$y = 17999x + 0.0114$	0.9975

λ_{max} = maximum wavelength.

occurred with the release of the drug, which was adsorbed onto the surface of the nanoparticles, and controlled release, which was caused by the diffusion of the drug into the nanoparticles.¹⁹ More than 30 wt % of NIF was released from the PCNs at pH 7.4 within 1 h, whereas about 4 h was needed for more than 30 wt % of the drug to be released at pH 1.2 and 2.0. It seemed that the release profile showed an initial burst release; this corresponded to a significant amount of drug initially associated with nanoparticles remaining on the surface because of the interaction forces between CS, PLA, and NIF. In comparison to the microsphere loading of NIF,^{3,6} the NIF released from PCNs could be controlled more easily.

Effect of the drug loading. The drug-release data in Figure 6 for PCNs loaded with high amounts of NIF (30 and 50 wt %) displayed higher NIF release contents than the samples containing small amounts of NIF (10 and 20 wt %). A similar phenomenon was also observed for the release of lamivudine from PCs loaded with lamivudine¹³ and BMP-2-derived synthetic peptide from PLA/chitosan microspheres (CMs).¹⁵ It was clear that the drug loading had a slight effect on the drug-release rate.⁴ Here, the prolonged drug release was observed for the formulation containing the lower amount of NIF. The release rate became much slower with the lower amount of drug in the nanoparticles because of the availability of more free void spaces, through which a lesser number of drug molecules could be transported. In addition, the lower crystallinity at the high NIF content (as mentioned in the XRD section) also influenced a high release rate of NIF from the PCNs.

Kinetics Study

To our knowledge, there were some different types of drug-release kinetics and mechanisms based on the polymer matrices. Drug release from matrices usually implies water penetration into the matrix, hydration, swelling, diffusion of the dissolved drug, and/or the erosion of the gelatinous layer.^{2–7,11,14,15,21,22} It is worth mentioning that the release mechanism of a drug depends on the drug dosage, investigated pH solution, nature of the drug, and the polymer used.^{14,15} Recently, the most probable kinetics have been used for the drug release, as depicted later:

$$\text{Zero-order kinetics: } W_t = W_0 + k_1 t \quad (1)$$

$$\text{First-order kinetics: } \log C = \log C_0 - k_2 t / 2.303 \quad (2)$$

$$\begin{aligned} &\text{Hixson-Crowell cube-root equation (Erosin model):} \\ &(100 - W)^{1/3} = 100^{1/3} - k_3 t \quad (3) \end{aligned}$$

$$\begin{aligned} &\text{Higuchi square root of time equation (diffusion model):} \\ &W = k_4 t \quad (4) \end{aligned}$$

$$\begin{aligned} &\text{Power law equation (diffusion/relaxation model):} \\ &M_t / M_\infty = k_5 t^n \quad (5) \end{aligned}$$

Where W_0 and W_t is amount of drug released at a time initial and t ; k (k_1, k_2, k_3, k_4, k_5) is constant release; n is diffusional constant; C_0 and C_t are concentration of drug at time initial and t , respectively; M_t / M_∞ is the fractional drug release into dissolution medium. The n characterized the drug release transport mechanism. When $n \leq 0.5$ and $n = 0.5$, the drug diffusion

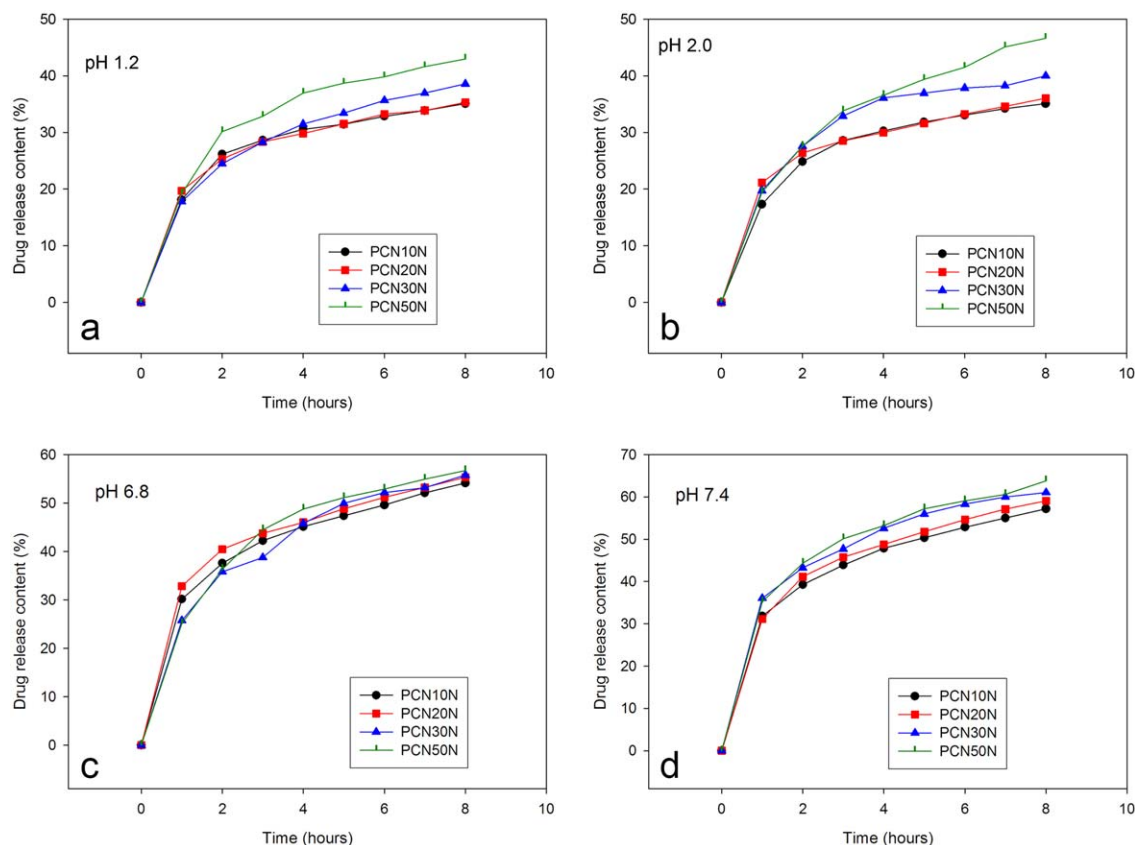


Figure 6. *In vitro* NIF release content from the PCNs versus time. [Color figure can be viewed in the online issue, which is available at wileyonlinelibrary.com.]

Table IV. k and R^2 Values of Zero-Order Kinetic, First-Order Kinetic, Hixson–Crowell Cube-Root, Higuchi Square Root of Time, and Power Law Equations of PCNs at pH 7.4

Sample	Zero-order kinetics		First-order kinetics		Hixson–Crowell cube root		Higuchi square root of time		Power law		
	k_1	R^2	k_2	R^2	k_3	R^2	k_4	R^2	k_5	n	R^2
PCN10N	0.00003	0.9467	0.0317	0.7181	0.0019	0.9182	0.0134	0.9906	0.779	0.279	0.9988
PCN20N	0.00008	0.9786	0.0584	0.8558	0.0020	0.9172	0.0306	0.9958	0.728	0.342	0.9948
PCN30N	0.00009	0.9334	0.0924	0.8338	0.0025	0.9097	0.0389	0.9747	0.797	0.261	0.9958
PCN50N	0.0138	0.9183	0.1006	0.6316	0.0036	0.8219	0.0553	0.9769	0.784	0.276	0.9918

Table V. k , n , and R^2 Values of the Power Law Equation of the PCNs in Solutions of Different pH

Sample	pH 6.8			pH 2.0			pH 1.2		
	k_5	n	R^2	k_5	n	R^2	k_5	n	R^2
PCN10N	0.781	0.274	0.9960	0.764	0.322	0.9509	0.778	0.293	0.9392
PCN20N	0.801	0.242	0.9938	0.800	0.244	0.9913	0.791	0.258	0.9790
PCN30N	0.716	0.375	0.9807	0.761	0.313	0.9516	0.733	0.339	0.9794
PCN50N	0.718	0.376	0.9669	0.688	0.405	0.9879	0.741	0.331	0.9309

from the polymer matrix corresponds to a Fickian diffusion mechanism and a quasi-Fickian diffusion mechanism, respectively. When $0.5 < n < 1$, an anomalous, non-Fickian drug diffusion occurs. When $n = 1$, a non-Fickian, case of II (relaxational) transport or zero-order release kinetics could be observed, and $n > 1$ corresponds to super case II transport.

To study the drug-release kinetics, the data obtained from *in vitro* drug-release test dealt with the previous kinetic equations. Drug-release constant (k) and R^2 calculated because of zero-order kinetic, first-order kinetic, Hixson–Crowell cube root, Higuchi square root of time, and power law equations of PCNs are presented in Table IV. Because of the R^2 value, the power law equation (diffusion/relaxation model) was the most appropriate for studying the NIF release kinetics from PCNs (all $R^2 > 0.991$). The values of k and n depended on the drug-loading content. Clearly, the NIF release-transport mechanism in pH 7.4 solution complied with the Fickian diffusion mechanism because of the value of $n \leq 0.5$. This mechanism also was observed for NIF release kinetics in other studies.^{3,6,7}

The k , n , and R^2 values of the power law equation of the PCNs in other pH solutions are presented in Table V. We observed that the NIF release-transport mechanism also complied with the Fickian diffusion mechanism, such as that in the pH 7.4 solution.

CONCLUSIONS

The most suitable preparation conditions, morphology, structure, crystallinity, and *in vitro* NIF release of PCNs were studied. The PCNs had average particle sizes in the range 100–400 nm; this depended on the preparation conditions. On the basis of the results of the particle size distribution of the PCNs prepared with different distilled water volumes, PEO contents, and PLA/CS ratios, the most suitable conditions for preparing PCNs were as follows: 250 mL of water, 400 mg of PEO, and a PLA/CS ratio of 2:1. FTIR analysis proved that NIF was carried by PCs and interacted with PLA and CS. The FESEM images of the PCs and PCN20N showed that these samples had basic particle sizes from 20 to 40 nm, but they were agglomerated together to form bigger particle sizes. The XRD data showed that the crystallinity of the PCNs was higher than that of the PCs. The calibration equations of NIF in different pH solutions were set up to calculate the NIF release content from the PCNs. The drug was released from PCNs in a controlled manner. We observed that the drug-release content from the PCNs with loadings of 10–50 wt % NIF in the basic medium was higher than that in the acidic medium. On the basis of the calculation of the kinetic parameters of drug release according to different models, the probable drug-release mechanism complied with the Fickian diffusion mechanism.

ACKNOWLEDGMENTS

This work was financially supported by the Vietnam National Foundation for Science and Technology Development (contract grant number DT.NCCB-DHUD.2012-G/09).

REFERENCES

1. Varshosaz, J.; Dehghan, Z. *Eur. J. Pharm. Biopharm.* **2002**, *54*, 135.
2. Filipović-Grčić, J.; Bećirević-Laćan, M.; Škalko, N.; Jalšenjak, I. *Int. J. Pharm.* **1996**, *135*, 183.
3. Huang, J.; Wigent, J. R.; Bentzley, M. C.; Schwartz, B. J. *Int. J. Pharm.* **2006**, *319*, 44.
4. Guyot, M.; Fawaz, F. *Int. J. Pharm.* **1998**, *175*, 61.
5. Praveen, B. K.; Lata, S. M.; Tejraj, M. A. *Polym. Bull.* **2013**, *70*, 3387.
6. Namdev, B. S.; Tejraj, M. A. *Int. J. Pharm.* **2007**, *345*, 51.
7. Vijay, K. S.; Namdev, B. S.; Prasannakumar, S.; Sherigara, B. S.; Tejraj, M. A. *J. Polym. Res.* **2011**, *18*, 359.
8. Jeevitha, D.; Kanchana, A. *Colloids Surf. B* **2013**, *101*, 126.
9. Yan, S.; Changsheng, L.; Yuan, Y.; Xinyi, T.; Fan, Y.; Xiaoqian, S.; Huanjun, Z.; Feng, X. *Biomaterials* **2009**, *30*, 2340.
10. Xu-Bo, Y.; Yan-Bo, Y.; Wei, J.; Jie, L.; En-Jiang, T. *Int. J. Pharm.* **2008**, *349*, 241.
11. Nanda, R.; Sasmal, A.; Nayak, P. L. *Carbohydr. Polym.* **2011**, *83*, 988.
12. Prabakaran, M.; Rodriguez-Perez, M. A.; de Saja, J. A.; Mano, J. F. *J. Biomed. Mater. Res. B* **2007**, *81*, 427.
13. Dev, A.; Binulal, N. S.; Anitha, A.; Nair, S. V.; Fruike, T.; Tamura, H.; Jayakumar, R. *Carbohydr. Polym.* **2010**, *80*, 833.
14. Rajan, M.; Raj, V. *Carbohydr. Polym.* **2013**, *98*, 951.
15. Xufeng, N.; Qingling, F.; Mingbo, W.; Xiaodong, G.; Qixin, Z. *Polym. Degrad. Stab.* **2009**, *94*, 176.
16. Işıklan, N.; İnal, M.; Kurşun, F.; Gül den, E. *Carbohydr. Polym.* **2011**, *84*, 933.
17. Patitapabana, P.; Subash, C. M.; Subhashree, S.; Ajit, B.; Bibhukalyan, P. N. *J. Pharm. Anal.*, to appear.
18. Silverajah, V. S. G.; Ibrahim, N. A.; Zainuddin, N.; Wan, M.; Yunus, W.; Hassan, H. A. *Molecules* **2012**, *17*, 11729.
19. Ioelovich, M. *Res. Rev. J. Chem.* **2014**, *3*, 7.
20. Huh, K. M.; Lee, S. C.; Cho, Y. W.; Lee, J.; Jeong, J. H.; Park, K. *J. Controlled Release* **2005**, *101*, 59.
21. Hui, Y. Z.; Pei, P. C.; Jun, B. L.; Fa, L. Z.; Pei, P. D. *J. Appl. Polym. Sci.* **2015**, *132*, 42152.
22. Feng, C.; Jing, G.; Lu, W.; Xingyou, H. *J. Appl. Polym. Sci.* **2015**, *132*, 42060.